HHS Public Access

Author manuscript

Cytotherapy. Author manuscript; available in PMC 2022 April 01.

Published in final edited form as:

Cytotherapy. 2021 April ; 23(4): 301–310. doi:10.1016/j.jcyt.2020.09.008.

Minor Salivary Gland Mesenchymal Stromal Cells Derived From Patients With Sjögren's Syndrome Deploy Intact Immune Plasticity

Sara S. McCoy, MD[1], **Jayeeta Giri, PhD**[2], **Rahul Das, PhD**[2], **Pradyut K. Paul, PhD**[2], **Andrea Pennati, PhD**[2], **Maxwell Parker**[1], **Yun Liang, PhD**[3], **Jacques Galipeau, MD**[2]

[1]Department of Medicine, University of Wisconsin School of Medicine and Health, Madison, USA

[2]Department of Medicine, University of Wisconsin Carbone Comprehensive Cancer Center, University of Wisconsin, Madison, USA

[3]Department of Medical Biology and Immunology, University of Wisconsin, Madison, USA.

Abstract

Objective: Mesenchymal stromal cells (MSCs) provide minor salivary glands (MSGs) with support and niche cells for epithelial glandular tissue. Little is known about resident MSG derived MSCs (MSG-MSCs) in primary Sjögren's syndrome (pSS). Our objective is to define the immunobiology of endogenous pSS MSG-MSCs.

Methods: Using culture adapted MSG-MSCs isolated from consenting pSS subjects (n=13), we performed *in vitro* interrogation of pSS MSG-MSC immunobiology and global gene expression compared to controls. To this end, we performed phenotypic and immune functional analysis of indoleamine 2,3-dioxygenase (IDO), programmed death-ligand 1 (PD-L1), and intercellular adhesion marker-1 (ICAM-1) before and after interferon (IFN)γ licensing as well as the effect of MSG-MSCs on T cell proliferation. Considering the female predominance of pSS, we also addressed the influence of 17 β-estradiol on estrogen receptorα^{+}-related MSC function.

Results: We found that MSG-MSCs deploy normal immunoregulatory functionality after IFNγ stimulation as demonstrated by increased protein-level expression of IDO, PD-L1, and ICAM-1. We also found that MSG-MSCs suppressed T cell proliferation in a dose-dependent manner independent of 17 β-estradiol exposure. Gene ontology and pathway analysis highlighted extracellular matrix deposition as a possible difference between pSS and control MSG-MSCs. MSG-MSCs demonstrate increased αSMA expression in pSS indicating a partial myofibroblast-like adaptation.

Corresponding author Sara S. McCoy, MD, University of Wisconsin, School of Medicine and Public Health, 1685 Highland Avenue, Madison, WI 53705-2281, ssmccoy@medicine.wisc.edu.

Declarations of interest: none

Conclusions: These findings establish similar immunoregulatory function of MSG-MSCs in both pSS and control patients precluding intrinsic MSC immune regulatory defects in pSS. pSS MSG-MSCs show a partial imprinted myofibroblast-like phenotype which may arise in the setting of chronic inflammation, providing a plausible etiology for pSS related glandular fibrosis.

Keywords

Mesenchymal Stromal Cells; Primary Sjögren's Syndrome; Minor Salivary Gland; Myofibroblast

INTRODUCTION

Primary Sjögren's syndrome (pSS) is the second most common systemic autoimmune disease with characteristic features of oral and ocular sicca. Oral sicca (xerostomia) associated with pSS leads to marked reduction in quality of life and increased dental caries and dental care cost.(1–4) Despite the profound impact of xerostomia on pSS patients, therapy is limited to symptomatic treatments like topical wetting agents or sialagogues.

pSS causes xerostomia through the hallmark clinical and pathogenic features of salivary gland inflammation and, ultimately, fibrosis.(5) The stromal component of salivary glands is partially comprised of mesenchymal stromal cells (MSCs), providing tissue homeostatic properties including regeneration, repair and immune modulation. Endogenous salivary gland MSCs are an ideal target of study in pSS because salivary gland health is dependent on resident MSCs.(6) MSCs reduce inflammation by acting as immunomodulators and promote tissue regeneration.(7, 8)

Despite the prominent role of MSCs as immunomodulating cells, little is known about pSS resident salivary gland MSCs immune functionality. pSS salivary gland MSCs have been found to have impaired differentiation potential and reduced regenerative capacity compared to control salivary gland MSCs, however the impact of pSS salivary gland MSCs on local immunobiology is unknown.(6, 9) The objective of this study is to define the immunobiology of culture-adapted MSCs derived from endogenous salivary minor salivary gland (MSG)-MSCs. To our knowledge, this is the first study to report on the immunomodulatory properties of human MSG-MSCs.

METHODS

Patient Recruitment and MSC Isolation

We obtained informed consent from subjects during MSG biopsy visits in compliance with the Helsinki declaration. pSS subjects met 2016 ACR/EULAR criteria.(10) Control patients recruited at the time of the MSG biopsy had normal serology (ANA ≤ 1:160 and negative anti-SSA antibody), focus score <1 on histopathology, and did not have a diagnosis of pSS, another autoimmune disease, HIV, or Hepatitis C. Thirteen pSS and 12 control subjects were recruited (Table 1).

To isolate MSG-MSCs, MSGs were collected from the recruited subjects, minced, and digested with 3 mg/mL collagenase type IV (Worthington, Lakewood, NJ) for 1 hour at 37°C.(11) The digested tissue was washed with HBSS, filtered through a 100 μM

strainer, spun, and re-suspended in complete media (α-minimal essential media (MEM, Corning, Tewksbury, MA), 20% fetal bovine serum (FBS, Sigma-Aldrich, St. Louis, MO), 1% L-Glutamine (Corning), and 1% Penicillin/Streptomycin (Lonza, Walkersville, MD). For estrogen treatment experiments, we used phenol-red free media (Thermo Fisher Scientific, Waltham, MA) and charcoal-stripped FBS (Sigma-Aldrich). All experiments were performed on MSG-MSCs between passage two and passage eight. CFU-F was calculated by plating 100 MSG-MSCs in six, T-75 flasks. After seven days, the number of colonies with ≥ 20 cells were counted and averaged.

Flow Cytometry

Fluorochrome conjugated human antibodies included: CD19-PE-Cy7 (BD Biosciences, San Jose, CA), CD73-Brilliant violet (BD Biosciences), CD90-APC (BD Biosciences), CD45-FITC (BD Biosciences), CD105-PE (BD Biosciences), HLA-DRPerCP (BD Biosciences), HLA-A,B,C-APC (BD Biosciences), indoleamine 2,3-dioxygenase (IDO)-PE (Thermo Fisher Scientific), CD54 (ICAM-1)-APC (BD Biosciences), and CD274 (PD-L1)-BV 421 (BD Bioscences). Intracellular staining of IDO and Ki-67 was performed using BD Cytofix/Cytoperm per the manufacturer's recommendations. Live/dead cells were determined using Ghost red 780 viability dye (Tonbo Biosciences, San Diego, CA). Flow cytometry using an Attune NxT Flow Cytometer (Thermo Fisher Scientific) and analyzed using FCS Express 7 flow cytometry software.

Adipogenic and Osteogenic Differentiation

We included insulin 1μL/mL (10μg/mL) (Sigma-Aldrich), dexamethasone 2μM/mL (Sigma-Aldrich), rosiglitazone 0.04μM/mL (Cayman chemicals, Ann Arbor, MI), and isobutylmethylxanthine 1mM/mL (Cayman Chemicals) in standard MSC media. Media was changed every three days and, after 14 days, Oil-red-O-staining was performed. We used StemPro™ Osteogenesis differentiation kit (ThermoFisher, Waltham, MA). We treated MSCs in standard media or with StemPro™ osteogenesis supplement for 21 days as per the recommended protocol. After 21 days, we fixed the cells and stained with Alizarin Red for imaging.

Co-culture of MSCs and Peripheral Blood Mononuclear Cells (PBMCs)

For the co-culture, MSG-MSCs were serum-starved for 24 hours using α-MEM with 1% FBS, then licensed for a further 24 hours in complete media with 10 ng/mL IFNγ or vehicle control. We added allogeneic donor PBMCs collected from normal volunteers at ratios of 1:10, 1:50, and 1:500 in standard culture conditions. We stimulated PBMCs by adding 2 μl/mL PHA (Invitrogen, Carlsbad, CA) to the co-culture. After four days, we performed T cell proliferation flow cytometry analysis using intracellular Ki-67 staining (BD Biosciences). We used anti-human CD3 antibody in order to identify T cells (Invitrogen).

Real time quantitative PCR

We performed RNA extraction using Direct-Zol RNA kit (Zymo Research, Irvine, CA) and nucleic acid quantification with Tecan's NanoQuant Plate™ reader (Baldwin

Park, CA). 500 ng of RNA was transcribed to complementary DNA using an Eppendorf thermocycler. PCR was performed on a Bio-Rad CFX96 Real-Time System (Hercules, CA) with the primers of interest. Primers included COL6A6 (Forward: 5′-CCCAGGCCACAGATTTCCAT-3′; Reverse: 5′-TCCCACCCATCTGCCTGATA-3′), COL22A1 (Forward: 5′-GTGATTGGCAAGCGCCTCTAC-3; Reverse: 5′-CAAGTCTCCAATTCTGCGTGTCTC-3′), GAPDH (Forward: 5'-GATTCCACCCATGGCAAATTC-3'; Reverse: 5'- GTCATGAGTCCTTCCACGATA C-3'). Cycle times, normalized to GAPDH, were graphed as fold-change expression of pSS MSG-MSCs over control MSG-MSCs using $2^{-\Delta\Delta CT}$.

Immunocytochemistry

MSG-MSCs were grown to 80% confluence, fixed in 4% PFA, blocked with normal goat serum for one hour, then incubated with αSMA unconjugated mouse anti-human primary antibody at 4°C overnight. We used secondary goat anti-mouse antibody staining with a conjugated Alexa Fluor Plus 555 antibody (Thermo Fisher Scientific). Counterstaining and slide fixation was performed using ProLong Diamond AntiFade Mountant with DAPI (Invitrogen). We acquired and analyzed images with a NikonA1RS confocal microscope and Nikon elements software, respectively. Average fluorescence per nuclei was performed. Images were combined into overlay for easy visualization.

Western Blot

Cell lysates were isolated from IFNγ- or estrogen-treated MSG-MSCs. We detected protein using primary rabbit antihuman α-Smooth Muscle Actin (SMA) (1:1000; Cell Signaling Technology, Danvers MA), rabbit antihuman GAPDH (Cell Signaling Technology), or rabbit antihuman estrogen receptor alpha (Cell Signaling Technology) and horseradish peroxidase-coupled secondary antibodies (1:10,000; Bethyl Laboratories, Montgomery, TX). Blotted proteins were visualized using enhanced chemiluminescence (ECL; Amersham, UK)

RNA library preparation and RNA-Seq analysis

Transcriptomic analysis of independent biologic replicates of control and pSS (n=3 each) MSG-MSC lines was carried out by MedGenome, Inc (Foster City, CA) for a total of 12 samples (n=3 control-treated and -untreated; n=3 pSS-treated and untreated). Samples were serum starved for 24 hours then treated with or without estrogen 10^{-8}M for 24 hours. After RNA isolation, the library was generated by Illumina TruSeq Stranded RNA Library Prep Kit and NovaSeq sequencer. FastQC (version0.11.8) was used for data quality check. Based on quality reports, sequence reads were trimmed to retain high quality sequences for additional analysis. Alignment was performed with STAR aligner (version2.7.3a) and raw read counts were estimated with HTSeq (v0.11.2) and normalized with DESeq2. The aligned reads were used to estimate expression of genes with cufflinks (version2.2.1). Differential expression with fold change was performed with and without shrinkage.(12)

Gene ontology (GO) and pathway enrichment analysis

DAVID 6.8 online tool was used to evaluate GO of differentially expressed genes (website: https://david-d.ncifcrf.gov/).(13, 14) GO terms for biological process, cellular

component ,and molecular function, were identified for genes significantly differentially expressed using the adjusted p-value (Benjamin-Hochberg). Graphite website (https://graphiteweb.bio.unipd.it/) was used for Signaling Pathway Impact Analysis (SPIA) on the significantly differentially expressed genes.(15) SPIA provides a topologic pathway analysis by considering the amount of expression change of each gene, the differentially expressed gene position in the pathway, the topology of the pathway, and the type of gene interaction to identify pathways significantly impacted and to calculate the total net accumulated perturbation of the pathway.(16) SPIA topologies were derived from KEGG and Reactome databases.

Total Collagen Detection

Collagen concentration was determined using Sirius Red Collagen Detection Kit (Chondrex, Redmond, WA) in accordance with the manufacturer's instructions. pSS and control (n=6 each) samples were used for analysis. Conditioned medium collected at passage two for all MSG-MSCs was diluted 50% with PBS per manufacturer recommendations.

Statistical Analysis

For continuous and categorical variable comparisons we used two-tiered unpaired Student's t-test and Chi-squared testing, respectively. Statistical analysis was carried out by GraphPad Prism software (Graphad, Software, L Jolla, CA). p-values <0.05 were defined statistically significant.

RESULTS

Phenotypic characterization of MSG-MSCs derived from pSS subjects

MSG-MSCs had a CFU-F of 93% ± a standard deviation (SD) of 7%. The average doubling time of MSG-MSCs was 3.9 days (SD 1.5 ± days). MSC identity was verified as recommended by the International Society of Cell Therapy guidelines.(17) MSCs demonstrate three key features: i) plastic adherent in standard culture conditions, ii) express surface marker patterns including CD73, CD90, and CD105 but lacking CD45, CD34, CD14 or CD11b, CD79α or CD19, and HLA-DR, and iii) MSCs should demonstrate the ability to terminally differentiate to adipocytes, chondrocytes, or osteocytes. Morphologically, MSG-MSCs were plastic adherent (Figure 1A). Flow cytometry confirmed the upregulation of CD73, CD90, and CD105 and the downregulation of CD45, CD19, and HLA DR (Figure 1B & C). We also confirmed the presence of MHC class I (Supplemental Figure 1). No differences were noticeable for the surface markers expression between pSS and control MSG-MSCs. Finally, MSCs differentiate to adipocytes under adipogenic induction conditions and to osteocytes under osteocyte induction conditions (Figure 1D & 1E). Taken together, these data confirm that the cells isolated from minor salivary glands conform to standard definitions of MSC phenotype and that MSC phenotypic markers are similar between pSS and controls.

MSG-MSC immunomodulatory properties are intact in pSS and control samples

IFNγ treatment of MSCs promotes the characteristic *in vitro* immunosuppressive properties of MSCs.(18, 19) IFNγ upregulates key effectors of MSC-induced immunoregulation

including indoleamine 2,3-dioxygenase (IDO), intercellular adhesion marker (ICAM-1), and programmed death-ligand 1 (PD-L1), among others.(20–22) In order to establish the effect of IFNγ licensing on the immunobiology of MSG-MSCs, we treated pSS and control MSG-MSCs with IFNγ 25ng/mL. After 48 hours cells were harvested, stained for IDO, ICAM-1, and PD-L1 antibodies and evaluated with flow cytometry. We found that IFNγ licensing yielded statistically significant higher levels of IDO, ICAM-1, and PD-L1 expression comparable to MSCs from other tissue sources (Figure 2A, B &C).

MSCs regulate T cell function through several modalities including suppression of T cell proliferation.(23, 24) We sought to evaluate the functional impact of pSS and control MSG-MSCs on activated T cell proliferation with and without IFNγ stimulation. To address this question, we co-cultured IFNγ prelicensed MSG-MSCs (control and pSS) with PBMCs at 1:10, 1:50, and 1:500 ratio with PBMCs (MSCs:PBMCs) in RPMI with 10% FBS. PBMCs were stimulated with 2μl/mL PHA. Four days later, the PBMCs were collected for flow cytometry. MSG-MSCs exhibited dose-response relationships with $CD3^{+}Ki67^{+}$ T cell replication suppression (Figure 2D). Treatment with IFNγ did not enhance T cell suppression. pSS and control MSG-MSCs did not differentially inhibit T cell replication.

Estrogen does not impact the immunobiology of MSG-MSCs

pSS is a female predominant disease with peak onset during perimenopause, we thereby sought to determine whether estrogen, a key female sex hormone, alters MSG-MSC's immunomodulatory capacity.

To address this question, we first confirmed the presence of ERα in MSG-MSCs by western blot (Figure 3A). We then interrogated expression of IDO, ICAM-1, and PD-L1 in the presence and absence of 17 β-estradiol. We cultured MSG-MSCs in high (10^{-7}M) or low estrogen (10^{-9}M) conditions as defined by previous estrogenic studies.(25, 26) After 14 days, MSG-MSCs were treated with: 1) no estrogen, 2) high estrogen (10^{-7}M), or 3) low estrogen (10^{-9}M) for seven days. All MSG-MSCs were treated with IFNγ, harvested 14 hours later, stained for IDO, ICAM-1, and PD-L1, and evaluated by flow cytometry. IDO, ICAM-1, and PD-L1 expression was similar with and without estrogen exposure in pSS and control subjects (Figure 3C-E). We repeated the analysis in two male MSG-MSC cell lines to evaluate whether *in vivo* estrogen exposure affected *in vitro* results. We did not find any difference in IDO, ICAM-1, and PD-L1 after estrogen treatment (10^{-8}M) for 48 hours with subsequent IFNγ licensing for 48 hours compared to female cell lines (Supplemental Figure 2).

Transcriptomic profiling of pSS and control MSG-MSCs with and without estrogen exposure

All of the above studies prompted us to determine the differential gene expression between pSS and control MSG-MSCs and to further investigate a global view of estrogen impact on MSC gene expression.

pSS and control (n=3 biological replicates each) MSG-MSCs in both untreated and estrogen treated conditions were evaluated. Heat maps displayed differentially regulated genes filtered as follows: false discover rate (FDR) $p<0.1$ and log2 fold change >1 for upregulated

genes and <−1 for down regulated genes. The 22 differentially regulated genes between untreated pSS and control MSG-MSCs are displayed in heat maps (Figure 4A) (n=3 in each group).

We performed GO analysis on differentially regulated genes categorized by biologic processes, cellular component, and molecular function. The top three clusters of differentially regulated genes showed prominent role for extracellular matrix deposition among cellular components, biologic and molecular functions (Figure 4B). Pathway analysis showed a significantly inhibited extracellular matrix organization pathway (Figure 4C). Both the GO and pathway analysis supported a role for extracellular matrix activation in the pathogenesis of pSS in MSG-MSCs.

Using an FDR of $p<0.1$, no genes were differentially regulated between pSS MSG-MSCs with and without estrogen treatment. Overall, these results support our previous conclusion that estrogen has no direct impact on the immunomodulatory capacity of MSG-MSCs in pSS.

pSS MSG-MSCs express more αSMA but similar level of collagen compared to control MSG-MSCs

Since our transcriptome analysis study indicates a possible role of pSS MSG-MSCs in extracellular matrix organization, we evaluated the expression of αSMA and collagen, myofibroblast-specific markers, at both transcriptional and translational level. αSMA protein expression more than 3.5 fold higher in pSS than control samples ($p=0.03$) (Figure 5A & B). To study collagen expression, we evaluated the most significantly differentially expressed collagen subtypes from our RNA-Seq: Col22A1 and Col6A6. We did not find a significant difference in RNA expression of either collagen subtype between control and pSS MSG-MSCs (Figure 5C). The total collagen level present in the conditioned media of MSG-MSCs derived from pSS and control MSG-MSCs revealed no significant differences as well (Figure 5D).

DISCUSSION

Minor salivary glands play a central role in the pathogenesis and clinical presentation of pSS. It is well established that an autoimmune T cell response against salivary epithelial cells is at the core of pSS pathology.(27, 28) Considering the significant structural and regenerative functionality of tissue resident MSCs, we know little about the immune plasticity of resident MSG-MSCs. MSG-MSCs are a salient cell-type in the setting of pSS given their ability to modulate the local immune system. We report that the immunomodulatory capacity of MSG-MSCs is comparable in pSS and control MSG-MSCs (Figure 6).

One of the modalities through which MSG-MSCs regulate T cell function is by the suppression of T cell proliferation.(23, 24, 29) Resting and IFNγ pre-licensed MSG-MSCs exhibit their immunoregulatory properties by the secretion of IDO, PD-L1, and ICAM-1. IDO is the rate-limiting enzyme of tryptophan metabolism where tryptophan is converted to kynurenine and subsequently kynurenine inhibits T cell proliferation.(23, 24) PD-L1

expression is also associated with MSC potency and ability to suppress T cell proliferation.(22) Similarly, ICAM-1 is also responsible for modulating the local immune environment.(30) We found pSS and control MSG-MSCs express similar levels of IDO, PD-L1, and ICAM-1, with increased expression following IFNγ licensing. MSG-MSCs also suppress T cell proliferation in a dose dependent manner. Interestingly, we did not find that IFNγ licensing augments the ability of MSG-MSCs to inhibit T cell proliferation. It is possible that the PHA induced IFNγ production from PBMCs and blunted the effect of IFNγ pre-treatment. Alternatively, the effects of IFNγ pre-treatment could have been lost over the four days between PHA treatment and cell harvest. Finally, IFNγ pre-treatment might not impact the MSG-MSC ability to suppress T cell proliferation. Overall, these findings support the idea that the immunomodulatory capacity in both pSS and control MSG-MSCs is preserved. In contrast, other studies have highlighted differences in phenotype and function between pSS and control salivary gland MSCs.(6, 9) pSS MSG-MSCs have reduced AMY1, AQP5, and ZO-1 expression and reduced differentiation capacity and colony forming unit efficiency compared to controls.(9) Within the parotid gland, salivary gland MSCs are less frequent, have reduced ability to differentiate, and demonstrate increased senescence.(6) Increased senescence is theorized to be due to early mitotic stimulation and subsequent telomere shortening.(6) Therefore, it is possible that pSS MSG-MSCs could have a reduced *in vivo* local immunomodulatory impact due to numbers or early senescence, but not functional capacity. Finally, because control MSG-MSCs were obtained from a population with sicca symptoms and signs, we might have had reduced ability to detect a difference. However, determining the difference between MSG-MSCs from pSS versus sicca-controls has intrinsic value because these entities have similar presentations but different pathogenic mechanisms.

GO and pathway analysis of RNA-Seq data identified extracellular matrix deposition as a biologically plausible difference between pSS and control MSG-MSCs. Because MSG tissue in pSS demonstrates advanced fibrosis independent of age, we sought to evaluate whether MSG MSCs had a myofibroblast-like phenotype.(5) In other disease states, such as systemic sclerosis, MSCs can differentiate into myofibroblast-like cells.(31) Myofibroblast-like MSCs have also been identified to have a pathogenic role in other disease processes including renal and lung fibrosis.(32, 33) Myofibroblast-like MSCs have increased αSMA and collagen expression.(31) We found a partial myofibroblast-like phenotype with significantly increased αSMA protein expression in pSS MSG-MSCs but not increased collagen expression. It is possible that *in vivo*, MSG-MSCs could be exposed to higher levels of TGFβ in pSS compared to controls, driving a myofibroblast-like phenotype. However this hypothesis is less likely because the data on TGFβ presence in salivary glands is conflicting showing TGFβ could be increased, decreased or similar between pSS and control salivary glands.(34–38) Alternatively, the WNT/β-catenin signaling pathway, downstream of TGFβ, could be involved in formation of a myofibroblast-like cell and alter the immune system. Inhibition of the WNT/ β - catenin signaling pathway in lung resident MSCs abrogates TGFβ-induced conversion of MSCs to myofibroblasts.(39) WNT/β-catenin genes *LRP5, FRZB,* and *ADIPOQ*, are associated with increased risk of pSS.(40) WNT/β-catenin signaling also effects regulatory T-cell development and activation, Th17 balance, B cell development, and maturation of dendritic cells.(41) Thus aberrant WNT/β-catenin signaling is another plausible explanation for MSG-MSC myofibroblast-like cells and autoimmunity

in pSS. Another potential *in vivo* exposure is bone morphogenetic protein 6 (BMP6), which is expressed in higher levels in SS patients compared to controls.(42) Interestingly, BMP6 treated murine submandibular gland MSCs have higher T cell proliferation rates, a process mediated by DNA binding protein ID1. BMP6 neutralizing antibody treated mice demonstrated improved salivary flow, inflammatory infiltrate, and cytokine profile. BMP6 is also associated with fibrosis in other diseases, providing another pathway to explain aberrant immunomodulation in SS and fibrosis.(43, 44) Other factors present in the MSG microenvironment could also alter *in vivo* MSG-MSC function. We interrogated culture adapted MSC-MSGs, which might differ from *in vivo* cell conditions and function.

Estrogen has been theorized to be involved in the pathogenesis of pSS because autoantibodies are present for years prior to disease onset, yet clinical presentation is delayed until perimenopause.(45, 46) Additionally, lifetime exposure to estrogen is lower in pSS than controls.(47) We therefore sought to determine if estrogen status altered MSG-MSC immunobiology. In other organ systems, estrogen is capable of modifying MSC function.(25, 48–54) We did not find any evidence that estrogen altered MSG-MSC immunobiology, a finding further supported by our RNA-Seq data lacking expression differences between estrogen treated and untreated pSS MSG-MSCs. It is possible that other sex hormones associated with menstruation, such as progesterone alter MSG MSC immunobiology. Although estrogen has a pleiotropic effect in general on the immune system, we did not find compelling evidence that estrogen alters the immunobiology of MSG-MSCs.(55)

In summary, we found that tissue resident MSG-MSCs can be successfully culture adapted and their immunobiological function remains intact. Despite thorough analysis, we did not find any significant functional differences between pSS and control MSG-MSCs suggesting that endogenous MSG-MSCs are unlikely to directly facilitate the autoimmune pathology of pSS due to immune regulatory loss-of-function. Considering the post-menopausal female overrepresentation in pSS pathology, we also did not identify an intersect gain or loss between ERα signaling and immune plasticity, suggesting sex discrepancy dose not arise from intrinsic sex-hormone driven MSC immune functionality. Interestingly, we found that pSS MSG-MSCs display a partial myofibroblast-like cell phenotype compared to control MSG-MSCs. This suggests epigenetic imprinting, which may skew the mesenchymal plasticity of MSG-MSCs and possibly arises from the chronic glandular inflammation from which they arise. In sum, there is no clear evidence that pSS MSG-MSCs display defective immune modulatory potential that would implicate them in the ontogeny of autoimmunity. However, their physiological response to chronic inflammation may lead to a maladapted response leading to glandular fibrosis as reflected in part by a myofibroblast-like phenotype of cultured progeny. This latter observation suggests that inhibiting the response of endogenous MSG-MSCs to MSG chronic inflammation cues may mitigate the maladapted MSC response leading to fibrosis and glandular loss of function.

Supplementary Material

Refer to Web version on PubMed Central for supplementary material.

Acknowledgements:

We thank Wei Zhang for his recommendations and contributions to our RNA-Seq analysis.

Funding: The project described was supported by the Clinical and Translational Science Award (CTSA) program, through the NIH National Center for Advancing Translational Sciences (NCATS) [grant UL1TR002373 and KL2TR002374] to SM and the NIH/NIDDK [R01DK109508] to JG. The content is solely the responsibility of the authors and does not necessarily represent the official views of the NIH. The authors have no financial or commercial support that could create potential conflict of interest.

Ethics approval: This study was approved by the University of Wisconsin Health Sciences IRB (IRB# 2018–1815)

References

1. Lopez-Jornet P, Camacho-Alonso F. Quality of life in patients with Sjogren's syndrome and sicca complex. J Oral Rehabil. 2008;35(12):875–81. [PubMed: 18976259]
2. Berman N, Vivino F, Baker J, Dunham J, Pinto A. Risk factors for caries development in primary Sjogren syndrome. Oral Surg Oral Med Oral Pathol Oral Radiol. 2019;128(2):117–22. [PubMed: 31196703]
3. Christensen LB, Petersen PE, Thorn JJ, Schiødt M. Dental caries and dental health behavior of patients with primary Sjögren syndrome. Acta Odontol Scand. 2001;59(3):116–20. [PubMed: 11501878]
4. Fox PC, Bowman SJ, Segal B, Vivino FB, Murukutla N, Choueiri K, et al. Oral involvement in primary Sjögren syndrome. J Am Dent Assoc. 2008;139(12):1592–601. [PubMed: 19047665]
5. Leehan KM, Pezant NP, Rasmussen A, Grundahl K, Moore JS, Radfar L, et al. Minor salivary gland fibrosis in Sjogren's syndrome is elevated, associated with focus score and not solely a consequence of aging. Clin Exp Rheumatol. 2018;36 Suppl 112(3):80–8.
6. Pringle S, Wang X, Verstappen G, Terpstra JH, Zhang CK, He A, et al. Salivary Gland Stem Cells Age Prematurely in Primary Sjogren's syndrome. Arthritis Rheumatol. 2018.
7. Aggarwal S, Pittenger MF. Human mesenchymal stem cells modulate allogeneic immune cell responses. Blood. 2005;105(4):1815–22. [PubMed: 15494428]
8. Galipeau J, Sensebe L. Mesenchymal Stromal Cells: Clinical Challenges and Therapeutic Opportunities. Cell Stem Cell. 2018;22(6):824–33. [PubMed: 29859173]
9. Wang SQ, Wang YX, Hua H. Characteristics of Labial Gland Mesenchymal Stem Cells of Healthy Individuals and Patients with Sjogren's Syndrome: A Preliminary Study. Stem Cells Dev. 2017;26(16):1171–85. [PubMed: 28537471]
10. Shiboski CH, Shiboski SC, Seror R, Criswell LA, Labetoulle M, Lietman TM, et al. 2016 American College of Rheumatology/European League Against Rheumatism Classification Criteria for Primary Sjogren's Syndrome: A Consensus and Data-Driven Methodology Involving Three International Patient Cohorts. Arthritis Rheumatol. 2017;69(1):35–45. [PubMed: 27785888]
11. Bakopoulou A, Leyhausen G, Volk J, Tsiftsoglou A, Garefis P, Koidis P, et al. Assessment of the impact of two different isolation methods on the osteo/odontogenic differentiation potential of human dental stem cells derived from deciduous teeth. Calcif Tissue Int. 2011;88(2):130–41. [PubMed: 21153807]
12. Love MI, Huber W, Anders S. Moderated estimation of fold change and dispersion for RNA-seq data with DESeq2. Genome Biol. 2014;15(12):550. [PubMed: 25516281]
13. Huang da W, Sherman BT, Lempicki RA. Systematic and integrative analysis of large gene lists using DAVID bioinformatics resources. Nat Protoc. 2009;4(1):44–57. [PubMed: 19131956]
14. Huang da W, Sherman BT, Lempicki RA. Bioinformatics enrichment tools: paths toward the comprehensive functional analysis of large gene lists. Nucleic Acids Res. 2009;37(1):1–13. [PubMed: 19033363]
15. Sales G, Calura E, Martini P, Romualdi C. Graphite Web: Web tool for gene set analysis exploiting pathway topology. Nucleic Acids Res. 2013;41(Web Server issue):W89–97. [PubMed: 23666626]
16. Tarca AL, Draghici S, Khatri P, Hassan SS, Mittal P, Kim J-s, et al. A novel signaling pathway impact analysis. Bioinformatics. 2008;25(1):75–82. [PubMed: 18990722]

17. Dominici M, Le Blanc K, Mueller I, Slaper-Cortenbach I, Marini F, Krause D, et al. Minimal criteria for defining multipotent mesenchymal stromal cells. The International Society for Cellular Therapy position statement. Cytotherapy. 2006;8(4):315–7. [PubMed: 16923606]

18. Ren G, Zhang L, Zhao X, Xu G, Zhang Y, Roberts AI, et al. Mesenchymal stem cell-mediated immunosuppression occurs via concerted action of chemokines and nitric oxide. Cell Stem Cell. 2008;2(2):141–50. [PubMed: 18371435]

19. Duijvestein M, Wildenberg ME, Welling MM, Hennink S, Molendijk I, van Zuylen VL, et al. Pretreatment with interferon-γ enhances the therapeutic activity of mesenchymal stromal cells in animal models of colitis. Stem Cells. 2011;29(10):1549–58. [PubMed: 21898680]

20. Chinnadurai R, Copland IB, Ng S, Garcia M, Prasad M, Arafat D, et al. Mesenchymal Stromal Cells Derived From Crohn's Patients Deploy Indoleamine 2,3-dioxygenase-mediated Immune Suppression, Independent of Autophagy. Mol Ther. 2015;23(7):1248–61. [PubMed: 25899824]

21. François M, Romieu-Mourez R, Li M, Galipeau J. Human MSC suppression correlates with cytokine induction of indoleamine 2,3-dioxygenase and bystander M2 macrophage differentiation. Mol Ther. 2012;20(1):187–95. [PubMed: 21934657]

22. Guan Q, Li Y, Shpiruk T, Bhagwat S, Wall DA. Inducible indoleamine 2,3-dioxygenase 1 and programmed death ligand 1 expression as the potency marker for mesenchymal stromal cells. Cytotherapy. 2018;20(5):639–49. [PubMed: 29548707]

23. Li X, Xu Z, Bai J, Yang S, Zhao S, Zhang Y, et al. Umbilical Cord Tissue-Derived Mesenchymal Stem Cells Induce T Lymphocyte Apoptosis and Cell Cycle Arrest by Expression of Indoleamine 2, 3-Dioxygenase. Stem Cells Int. 2016;2016:7495135. [PubMed: 27418932]

24. Li M, Sun X, Kuang X, Liao Y, Li H, Luo D. Mesenchymal stem cells suppress CD8+ T cell-mediated activation by suppressing natural killer group 2, member D protein receptor expression and secretion of prostaglandin E2, indoleamine 2, 3-dioxygenase and transforming growth factor-beta. Clin Exp Immunol. 2014;178(3):516–24. [PubMed: 25070361]

25. Fan JZ, Yang L, Meng GL, Lin YS, Wei BY, Fan J, et al. Estrogen improves the proliferation and differentiation of hBMSCs derived from postmenopausal osteoporosis through notch signaling pathway. Mol Cell Biochem. 2014;392(1–2):85–93. [PubMed: 24752351]

26. Soldin OP, Guo T, Weiderpass E, Tractenberg RE, Hilakivi-Clarke L, Soldin SJ. Steroid hormone levels in pregnancy and 1 year postpartum using isotope dilution tandem mass spectrometry. Fertil Steril. 2005;84(3):701–10. [PubMed: 16169406]

27. Abu-Helu RF, Dimitriou ID, Kapsogeorgou EK, Moutsopoulos HM, Manoussakis MN. Induction of salivary gland epithelial cell injury in Sjogren's syndrome: in vitro assessment of T cell-derived cytokines and Fas protein expression. J Autoimmun. 2001;17(2):141–53. [PubMed: 11591123]

28. Fujihara T, Fujita H, Tsubota K, Saito K, Tsuzaka K, Abe T, et al. Preferential localization of CD8+ alpha E beta 7+ T cells around acinar epithelial cells with apoptosis in patients with Sjögren's syndrome. J Immunol. 1999;163(4):2226–35. [PubMed: 10438965]

29. Di Nicola M, Carlo-Stella C, Magni M, Milanesi M, Longoni PD, Matteucci P, et al. Human bone marrow stromal cells suppress T-lymphocyte proliferation induced by cellular or nonspecific mitogenic stimuli. Blood. 2002;99(10):3838–43. [PubMed: 11986244]

30. Rubtsov Y, Goryunov K, Romanov A, Suzdaltseva Y, Sharonov G, Tkachuk V. Molecular Mechanisms of Immunomodulation Properties of Mesenchymal Stromal Cells: A New Insight into the Role of ICAM-1. Stem Cells Int. 2017;2017:6516854. [PubMed: 28761447]

31. Taki Z, Gostjeva E, Thilly W, Yaseen B, Lopez H, Mirza M, et al. Pathogenic Activation of Mesenchymal Stem Cells is induced by the Disease Microenvironment in Systemic Sclerosis. Arthritis Rheumatol. 2020.

32. Kim W, Barron DA, San Martin R, Chan KS, Tran LL, Yang F, et al. RUNX1 is essential for mesenchymal stem cell proliferation and myofibroblast differentiation. Proc Natl Acad Sci U S A. 2014;111(46):16389–94. [PubMed: 25313057]

33. Wang C, Gu S, Cao H, Li Z, Xiang Z, Hu K, et al. miR-877–3p targets Smad7 and is associated with myofibroblast differentiation and bleomycin-induced lung fibrosis. Sci Rep. 2016;6:30122. [PubMed: 27444321]

34. Mason GI, Hamburger J, Bowman S, Matthews JB. Salivary gland expression of transforming growth factor beta isoforms in Sjogren's syndrome and benign lymphoepithelial lesions. Mol Pathol. 2003;56(1):52–9. [PubMed: 12560464]
35. Kolkowski EC, Reth P, Pelusa F, Bosch J, Pujol-Borrell R, Coll J, et al. Th1 predominance and perforin expression in minor salivary glands from patients with primary Sjögren's syndrome. J Autoimmun. 1999;13(1):155–62. [PubMed: 10441181]
36. Fox PC, Brennan M, Di Sun P. Cytokine expression in human labial minor salivary gland epithelial cells in health and disease. Arch Oral Biol. 1999;44 Suppl 1:S49–52. [PubMed: 10414856]
37. Cauli A, Yanni G, Pitzalis C, Challacombe S, Panayi GS. Cytokine and adhesion molecule expression in the minor salivary glands of patients with Sjögren's syndrome and chronic sialoadenitis. Ann Rheum Dis. 1995;54(3):209–15. [PubMed: 7748018]
38. Kizu Y, Sakurai H, Katagiri S, Shinozaki N, Ono M, Tsubota K, et al. Immunohistological analysis of tumour growth factor beta 1 expression in normal and inflamed salivary glands. J Clin Pathol. 1996;49(9):728–32. [PubMed: 9038756]
39. Cao H, Wang C, Chen X, Hou J, Xiang Z, Shen Y, et al. Inhibition of Wnt/β-catenin signaling suppresses myofibroblast differentiation of lung resident mesenchymal stem cells and pulmonary fibrosis. Sci Rep. 2018;8(1):13644. [PubMed: 30206265]
40. Fernández-Torres J, Pérez-Hernández N, Hernández-Molina G, Martínez-Nava GA, Garrido-Rodríguez D, López-Reyes A, et al. Risk of Wnt/β-catenin signalling pathway gene polymorphisms in primary Sjögren's syndrome. Rheumatology (Oxford). 2020;59(2):418–25. [PubMed: 31302686]
41. Staal FJ, Luis TC, Tiemessen MM. WNT signalling in the immune system: WNT is spreading its wings. Nat Rev Immunol. 2008;8(8):581–93. [PubMed: 18617885]
42. Xu J, Su Y, Hu L, Cain A, Gu Y, Liu B, et al. Effect of Bone Morphogenetic Protein 6 on Immunomodulatory Functions of Salivary Gland-Derived Mesenchymal Stem Cells in Sjögren's Syndrome. Stem Cells Dev. 2018;27(22):1540–8. [PubMed: 30132383]
43. Yano R, Golbar HM, Izawa T, Sawamoto O, Kuwamura M, Yamate J. Participation of bone morphogenetic protein (BMP)-6 and osteopontin in cisplatin (CDDP)-induced rat renal fibrosis. Exp Toxicol Pathol. 2015;67(2):99–107. [PubMed: 25467747]
44. Gitelman SE, Kobrin MS, Ye JQ, Lopez AR, Lee A, Derynck R. Recombinant Vgr-1/BMP-6-expressing tumors induce fibrosis and endochondral bone formation in vivo. J Cell Biol. 1994;126(6):1595–609. [PubMed: 8089189]
45. Alamanos Y, Tsifetaki N, Voulgari PV, Venetsanopoulou AI, Siozos C, Drosos AA. Epidemiology of primary Sjogren's syndrome in north-west Greece, 1982–2003. Rheumatology (Oxford). 2006;45(2):187–91. [PubMed: 16332955]
46. Qin B, Wang J, Yang Z, Yang M, Ma N, Huang F, et al. Epidemiology of primary Sjogren's syndrome: a systematic review and meta-analysis. Ann Rheum Dis. 2015;74(11):1983–9. [PubMed: 24938285]
47. McCoy SS, Sampene E, Baer AN. Sjogren's Syndrome is Associated With Reduced Lifetime Sex Hormone Exposure: A Case-Control Study. Arthritis Care Res (Hoboken). 2019.
48. Ayaloglu-Butun F, Terzioglu-Kara E, Tokcaer-Keskin Z, Akcali KC. The effect of estrogen on bone marrow-derived rat mesenchymal stem cell maintenance: inhibiting apoptosis through the expression of Bcl-xL and Bcl-2. Stem Cell Rev. 2012;8(2):393–401.
49. Chen FP, Hu CH, Wang KC. Estrogen modulates osteogenic activity and estrogen receptor mRNA in mesenchymal stem cells of women. Climacteric. 2013;16(1):154–60. [PubMed: 22642912]
50. Chen HY, Zhang X, Chen SF, Zhang YX, Liu YH, Ma LL, et al. The protective effect of 17beta-estradiol against hydrogen peroxide-induced apoptosis on mesenchymal stem cell. Biomed Pharmacother. 2012;66(1):57–63. [PubMed: 22281292]
51. Shao B, Liao L, Yu Y, Shuai Y, Su X, Jing H, et al. Estrogen preserves Fas ligand levels by inhibiting microRNA-181a in bone marrow-derived mesenchymal stem cells to maintain bone remodeling balance. FASEB J. 2015;29(9):3935–44. [PubMed: 26062603]
52. Gao Y, Huang E, Zhang H, Wang J, Wu N, Chen X, et al. Crosstalk between Wnt/betacatenin and estrogen receptor signaling synergistically promotes osteogenic differentiation of mesenchymal progenitor cells. PLoS One. 2013;8(12):e82436. [PubMed: 24340027]

53. Veronesi F, Della Bella E, Torricelli P, Pagani S, Fini M. Effect of adipose-derived mesenchymal stromal cells on tendon healing in aging and estrogen deficiency: an in vitro co-culture model. Cytotherapy. 2015;17(11):1536–44. [PubMed: 26305076]

54. Wang M, Tan J, Coffey A, Fehrenbacher J, Weil BR, Meldrum DR. Signal transducer and activator of transcription 3-stimulated hypoxia inducible factor-1alpha mediates estrogen receptor-alpha-induced mesenchymal stem cell vascular endothelial growth factor production. J Thorac Cardiovasc Surg. 2009;138(1):163–71, 71.e1. [PubMed: 19577074]

55. Moulton VR. Sex Hormones in Acquired Immunity and Autoimmune Disease. Front Immunol. 2018;9:2279. [PubMed: 30337927]

HIGHLIGHTS

- Primary Sjögren's syndrome (pSS) minor salivary gland mesenchymal stromal cells (MSG-MSCs) have preserved immunomodulatory function
- 17 β-estradiol exposure does not alter MSG-MSC immunomodulatory function
- Primary Sjögren's syndrome MSG-MSCs demonstrate a partial myofibroblast-like phenotype

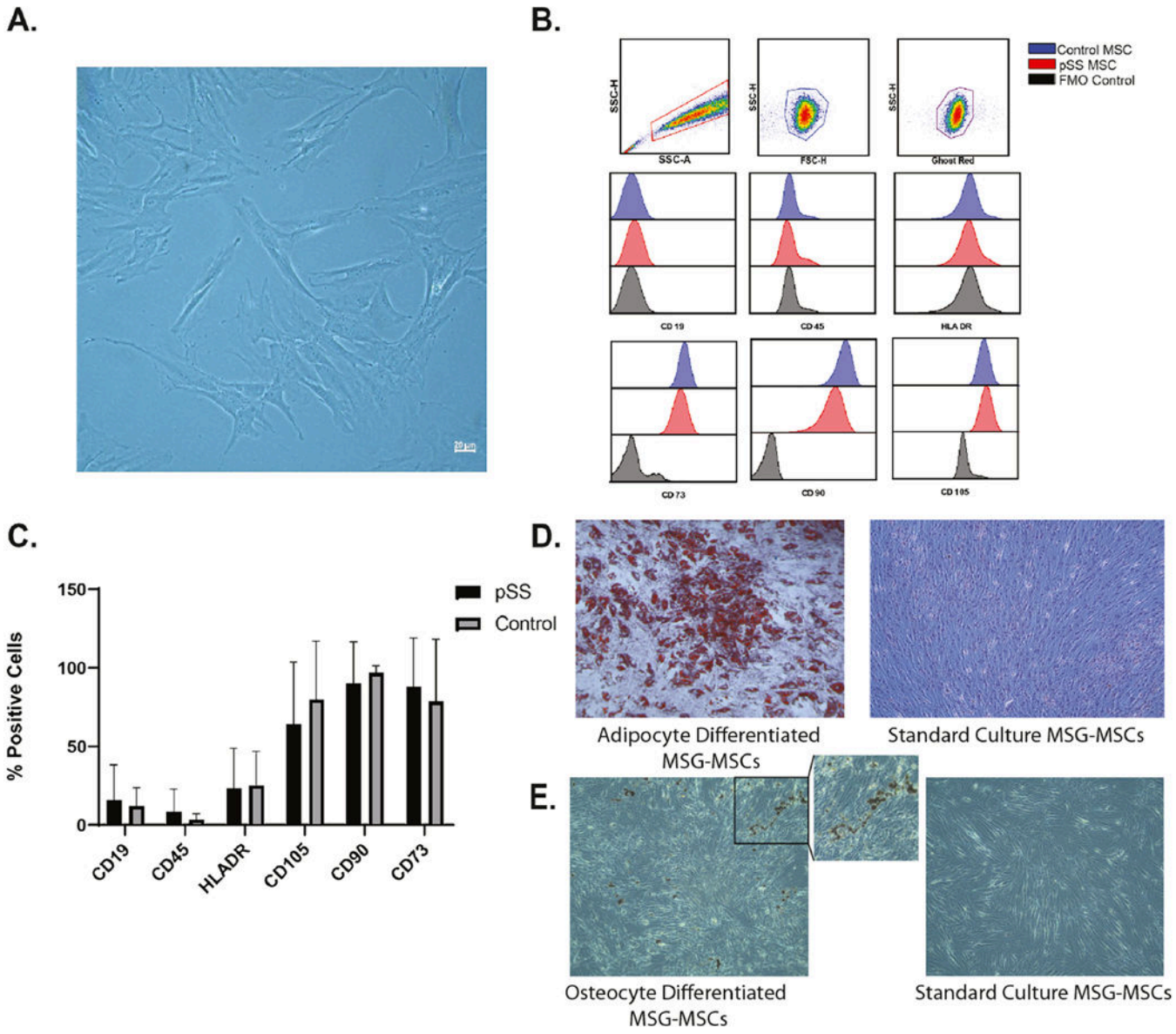

Figure 1.

Phenotypic characterization of MSG-MSCs derived from pSS and controls. A) Bright field microscopy picture of 20x MSG-MSC; B and C) Surface markers expression in pSS (n=8) and control (n=7) MSG-MSCs (CD45-, CD19-, and HLA DR- and CD105+, CD90+, and CD73+). Fluorescence minus one served as the control; D) Oil red-O-staining for adipogenic differentiation of MSG-MSCs and Oil-red-O-staining of MSG-MSCs cultured in standard conditions; E) Alizarin red staining for osteocyte differentiation of MSG-MSCs and alizarin red staining of MSG-MSCs cultured in standard conditions. Values are means ± SEM.

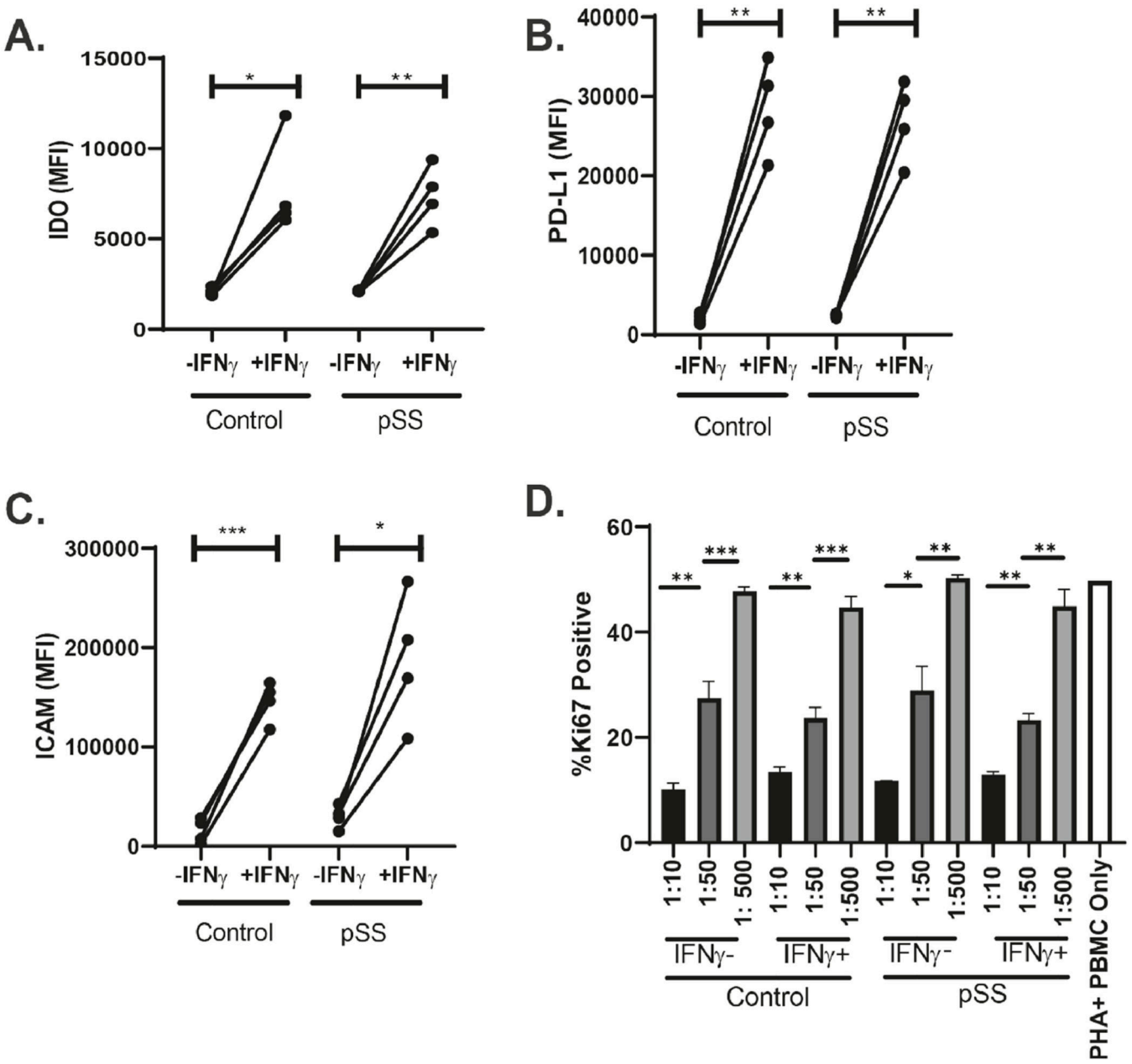

Figure 2.

MSG-MSC immunomodulatory properties are intact in pSS and controls pSS (n=3) and control (n=3) MSG-MSCs licensed with IFNγ (25 ng/mL) for 48 hours were harvested and stained with antibodies anti-IDO, PD-L1, and ICAM-1. Flow cytometry was performed after staining. Median fluorescence intensity (MFI) of MSC immunomodulatory markers A) IDO; B) PD-L1; C) ICAM-1; D) T cell suppression assay with MSG-MSCs with Ki-67 on pSS (n=3) and control (n=3). Values are means ± SEM. *=p<0.05, **=p<0.01, ***=p<0.001.

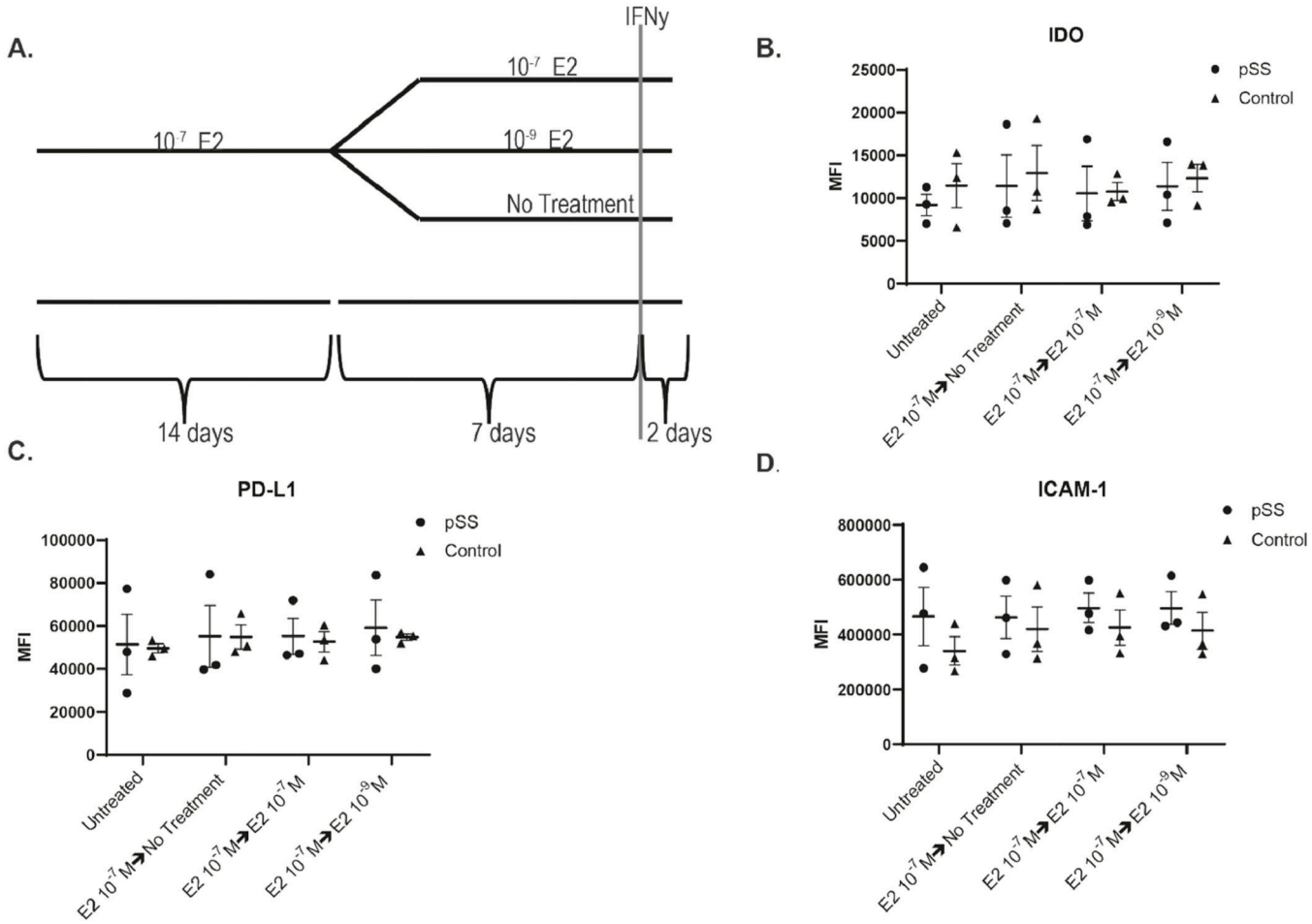

Figure 3.

Effect of estrogen exposure on pSS and control MSG-MSC's immunomodulatory capacity. pSS (n=3) and control (n=3) MSG MSCs were pre-treated with 10–7 M 17 β-estradiol (E2) for 14 days. After 14 days E2 doses included: none, 10–7μM, or 10–9 μM for 7 days. MSG-MSCs were then treated with IFNγ (25 ng/mL) for 48 hours. All experiments with estrogen were conducted using phenol red-free media and charcoal stripped FBS. MSG-MSCs were stained with antibodies anti-IDO, PD-L1, and ICAM-1 and flow cytometry analysis was carried out. A) Schematic representation of experimental conditions. B) Median fluorescence intensity of IDO; C) median fluorescence intensity of PD-L1; D) median fluorescence intensity of ICAM-1. Values are means ± SEM. *=p<0.05, **=p<.01, ***=p<.001.

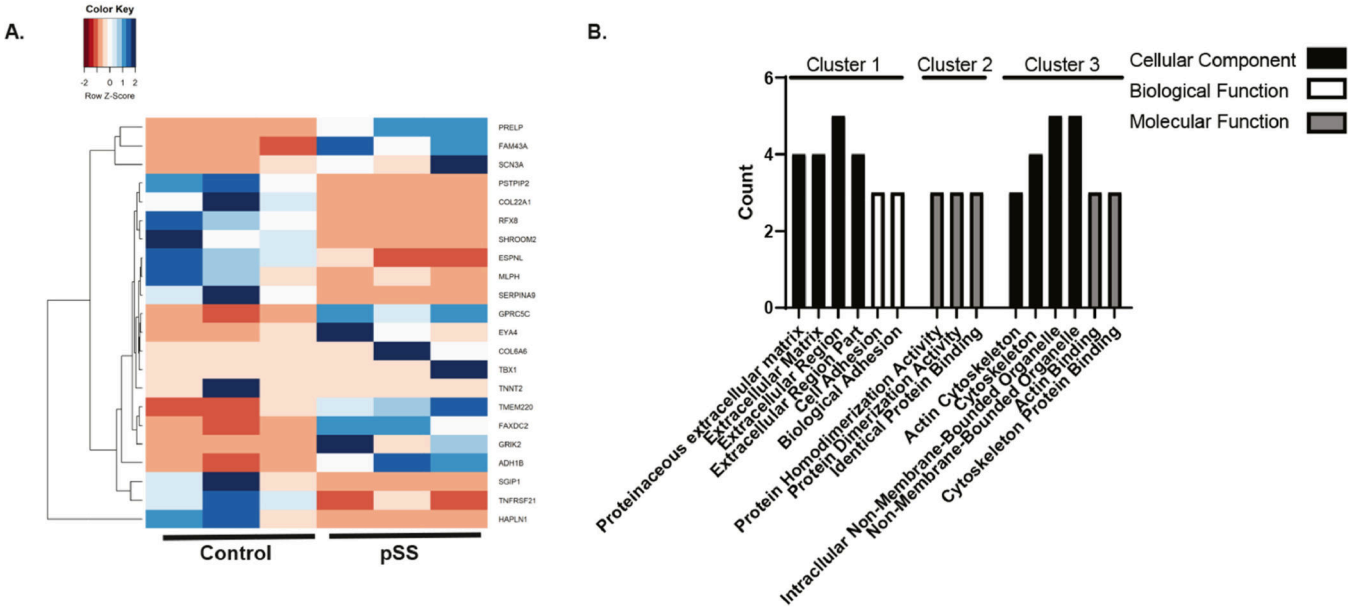

C. Pathways Identified by Signal Pathway Impact Analysis

Database	Pathway	pSize	NDE	pNDE	tA	pPERT	pG	pGFdr	pGFWER	Status
REACTOME	Extracellular matrix organization	90	2	0.0074	-1437	0.386	0.02	0.0918	0.31274	Inhibited
REACTOME	PPARA Activates Gene Expression	106	2	0.0101	0	1	0.057	0.0918	0.90503	Inhibited
REACTOME	Regulation of Lipid Metabolism by Peroxisome proliferator-activated receptor alpha (PPARalpha)	107	2	0.0103	0	1	0.057	0.0918	0.9185	Inhibited

Figure 4.

Transcriptomic profiling of pSS and control MSG-MSCs with and without estrogen exposure. MSG-MSCs were serum starved for 24 hours in 1% charcoal stripped FBS and phenol red-free α-MEM were then treated with or without 10–8 M 17 β-estradiol. After 24 hours, the cells were trypsinized and frozen. Untreated pSS (n=3) and control (n=3) and estrogen treated pSS (n=3) and control (n=3) MSG-MSC primary cell lines were evaluated. Heat maps displayed differentially regulated genes filtered with an adjusted p-value <0.1 and log2 fold change >1 for upregulated genes and <−1 for down regulated genes. Gene ontology and pathway analysis were performed on genes with an adjusted p-value<0.1. A) The top untreated pSS versus control differentially regulated genes are displayed in the heat map (Figure 4a); B) gene ontology analysis shows recurrent theme of extracellular matrix components to the differentially expressed genes; C) Signal Impact Pathway Analysis shows the only significant pathway to be activated extracellular matrix organization pathways. pSize=number of genes in the pathway; NDE=number of differentially expressed genes in the pathway; pNDE=hypergeometric probability of observing NDE differentially expressed genes in the pathway by chance; tA=observed value of the perturbation score; pPERT=bootstrap probability associated to tA; pG=combined probability of pNDE and pPERT; pGFDR=adjusted pG using False Discovery Rate correction; pGFWER=adjusted pG using Family Wise Error Rate (Bonferroni); Status=Inhibition or Activation according to the negative or positive sign of tA.

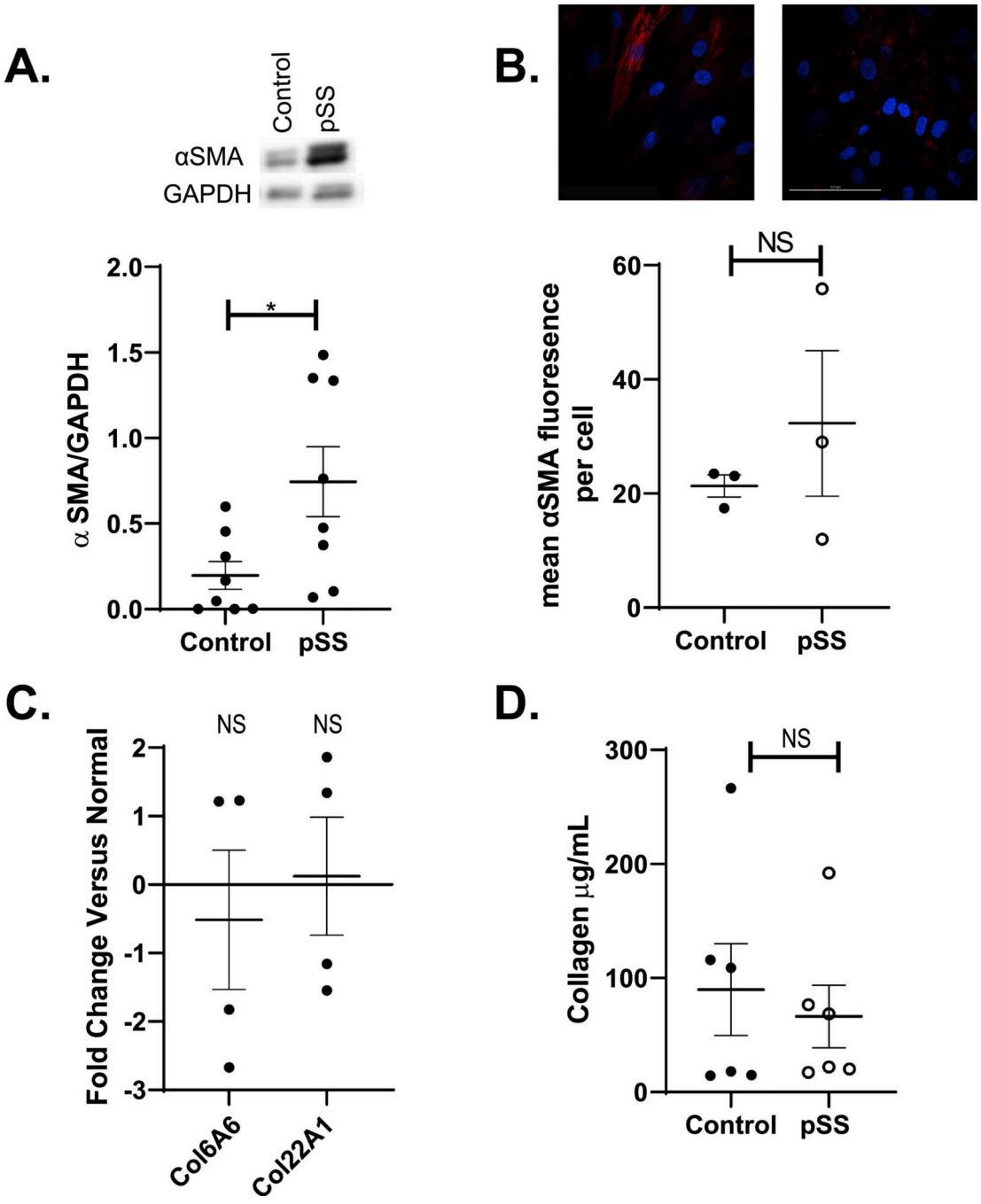

Figure 5.

Expression of αSMA and collagen in pSS and control MSG-MSCs. A) Proteins were isolated from MSG MSCs and western blot of eight control and eight pSS MSG-MSC samples was performed. αSMA expression of each sample relative to GAPDH loading control was estimated by densitometry analysis; B) Immunocytochemistry of three control and three pSS MSG-MSC primary cell lines. MSG-MSCs were serum starved in α-MEM and 1% FBS for 24 hours. Then MSG-MSCs were fixed and stained with antiαSMA unconjugated mouse antihuman primary antibody and microscopy was performed at 60x

with at least three images taken per slide. αSMA fluorescence was quantified using NIS elements software; C) Real-time PCR of COL6A6 and COL22A1 MSCs. Four pSS and four control samples were studied in triplicate. Each dot represents the average of the triplicate. Error bars represent standard error of the mean. Values are reported as fold change compared to normal. D) Total collagen μg/mL amounts from conditioned media from 6 pSS and 6 control samples, diluted 50% as per manufacturer's recommendations. Significance was calculated by ΔCT comparison using unpaired Student's t-test. Values are means ± SEM. *=p<0.05, **=p<.01, ***=p<.001, NS=non-significant.

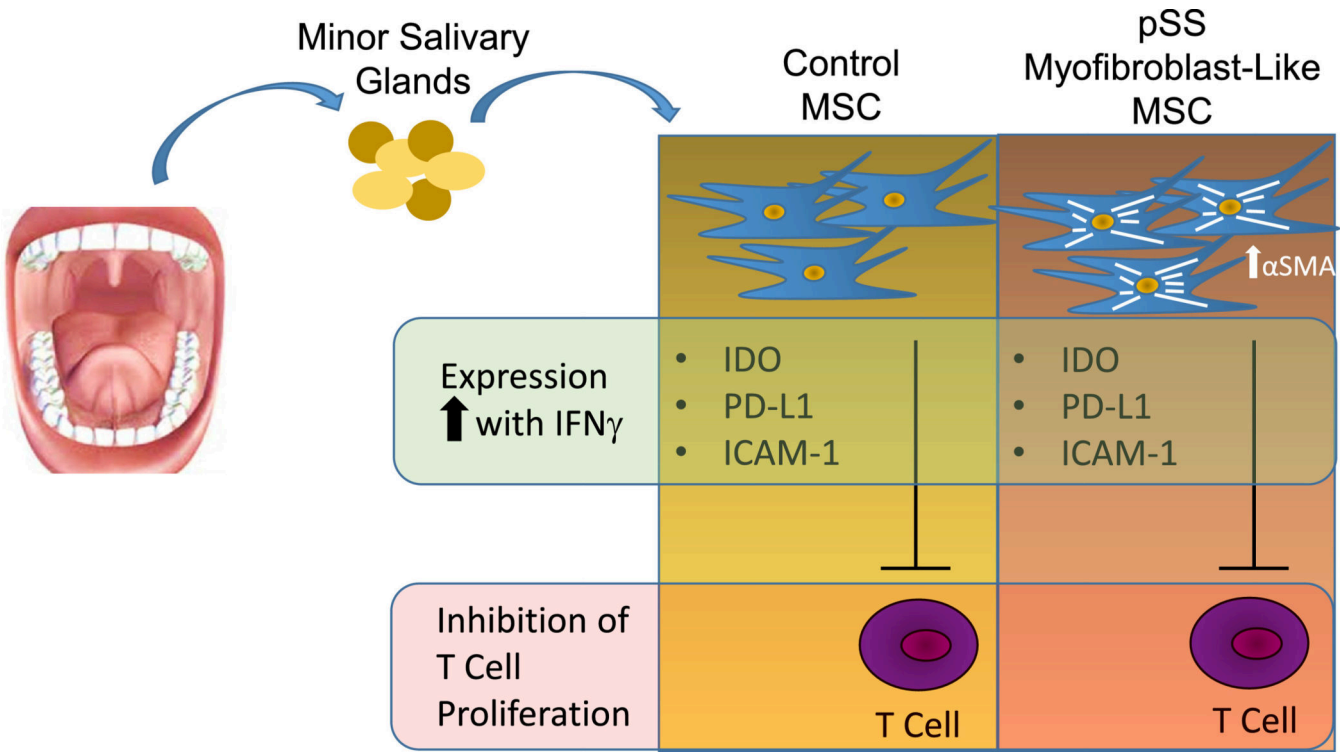

Figure 6.

Graphical abstract of intact immunomodulatory response of pSS and control MSG-MSCs. We establish similar immunoregulatory function of minor salivary gland mesenchymal stromal cells (MSG-MSCs) in both primary Sjögren's syndrome (pSS) and control patients precluding intrinsic MSC immune regulatory defects in pSS. pSS MSG-MSCs show a partial imprinted myofibroblast-like phenotype through increased αSMA, which may arise in the setting of chronic inflammation, providing a plausible etiology for pSS related glandular fibrosis.

Table 1.

Demographics of pSS and Control Subjects

Clinical characteristic	Control (n=12)	pSS (n=13)	p
Age (mean (SD))	51.1 (11.0)	49.6 (12.8)	0.8
Female n (%)	12 (100)	11 (85)	1.0
Caucasian n (%)	12 (100)	11 (85)	0.5
Former smoker n (%)	2 (17)	2 (15)	1.0
ANA >1:160 n (%)	n/a	7 (54)	
Anti-SSA antibody positive n (%)	n/a	13 (100)	
Focus score >1 n (%)	n/a	8 (62)	
Hypergammaglobulinemia n (%)	n/a	3 (23)	
Hypocomplementemia n (%)	n/a	2 (15)	